NJC

Accepted Manuscript

This is an *Accepted Manuscript*, which has been through the Royal Society of Chemistry peer review process and has been accepted for publication.

Accepted Manuscripts are published online shortly after acceptance, before technical editing, formatting and proof reading. Using this free service, authors can make their results available to the community, in citable form, before we publish the edited article. We will replace this *Accepted Manuscript* with the edited and formatted *Advance Article* as soon as it is available.

You can find more information about *Accepted Manuscripts* in the Information for Authors.

Please note that technical editing may introduce minor changes to the text and/or graphics, which may alter content. The journal's standard Terms & Conditions and the Ethical guidelines still apply. In no event shall the Royal Society of Chemistry be held responsible for any errors or omissions in this *Accepted Manuscript* or any consequences arising from the use of any information it contains.

ROYAL SOCIETY OF CHEMISTRY

www.rsc.org/njc

ARTICLE

Cite this: DOI: 10.1039/xoxxooooox

Received ooth January 2012,
Accepted ooth January 2012

DOI: 10.1039/xoxxooooox

www.rsc.org/

Hydrothermal Approach and Luminescent Properties for the Synthesis of Orthoniobates $GdNbO_4:Ln^{3+}$ (Ln = Dy, Eu) Single Crystals under High-Temperature High-Pressure Conditions

Min Yang[a], Xudong Zhao[a]*, Ying Ji[a], Fuyang Liu[a], Wei Liu[a], Jiayin Sun[b], Xiaoyang Liu[a]*

Single crystals $GdNbO_4:Ln^{3+}$ (Ln = Dy, Eu) phosphors were prepared *via* a high-temperature high-pressure hydrothermal procedure at 650 °C under the autogenous pressure. X-ray diffraction, field emission scanning electron microscopy, photoluminescence, Raman and XPS were utilized to characterize the synthesized phosphors. XRD reveals that the samples begin to crystalline at 550 °C and pure $GdNbO_4$ phase can be obtained at 650 °C. FE-SEM images indicate that $GdNbO_4:Ln^{3+}$ (Ln = Dy, Eu) samples consist of fine and sheet with a size 50-100 μm. Under the excitation of UV light, the $GdNbO_4:Eu^{3+}$ and $GdNbO_4:Dy^{3+}$ phosphors showed that the characteristic emission of Eu^{3+} is $^5D_0 \rightarrow {}^7F_J$ (J = 0,1,2,3,4), and Dy^{3+} ($^4F_{9/2} \rightarrow {}^6H_{15/2}$ and $^4F_{9/2} \rightarrow {}^6H_{13/2}$ transitions), respectively. The preparation method presented here dramatically lowered the traditional temperature of 2300 °C or above in Czochralski method. The $GdNbO_4:Dy^{3+}$ single crystals showed bright white emission under different excitation wavelengths with a relatively high quantum yield of 21.7%. The $GdNbO_4$: $0.05Eu^{3+}$ exhibited excellent bright red luminescence at 612 nm under near-UV excitation, narrowed emission spectra, room temperature luminescence lifetimes of milliseconds and maximum quantum efficiencies of 43.2%.

Introduction

Lanthanide orthoniobates have been extensively studied in recent years because of their environmental and energy related applications,[1, 2] which are based on their characteristic high chemical and electrochemical stabilities, photo-electronic activity, ion conductivity and luminescence.[3-6] For example, they can be used as phosphors for solid-state lighting,[7, 8] photo-catalysts for both contaminant degeneration and H_2 production,[9, 10 11]chemically robust hosts for nuclear materials and wastes, and ion conductors in lithium batteries or solid-oxide fuel cells.[12, 13] However, studies on $LnNbO_4$ compounds are limited due to the difficulty to grow their single crystals through traditional techniques, in which a crucible is demanded due to their aggressive melting reactivity and high melting points.[14-16]

Although $LaNbO_4$ and $NdNbO_4$ crystals were reported about three decades ago,[17] bulk crystals of $NdNbO_4$, $GdNbO_4$ and $HoNbO_4$ were only grown successfully with Czochralski method at temperature above 2300 ºC at the beginning of the last decade.[18] In 2008, Roof and his co-workers synthesized another two new niobates, $LaKNbO_6$ and Nd_2KNbO_6 effectively from molten hydroxides for the first time.[19, 20] Generally, there are just few niobates, especially, lanthanide niobates, synthesized at high temperature under high pressure (HTHP) up to present.

The hydrothermal process has been known to be one of the most important synthetic methods for niobates.[21] Aqueous solvents or mineralizers dissolve and recrystallize materials under high pressure at high temperature, which are relatively insoluble under ordinary conditions.[22-25] Additionally, this method is simple with low cost and very good product-morphology control.[26] Furthermore, compared with traditional solid method, the synthesis under high pressure has two prominent advantages: (1) The decrease of interatomic distances in existing materials; (2) densification effect during the synthesis of new materials, stabilization of precursors, compressing of the corresponding atoms to increase the reactivity.[27] Therefore, hydrothermal process under high pressure becomes an efficient way for many researchers to

obtain $LnNbO_4$ single crystals in this field. For example, Lii *et al*. reported that $Rb_2(VO)(Si_4O_{10})•XH_2O$ could be synthesized under 110 Mpa within 3 d at relatively low temperature of 550 ºC.[28] We have been interested in the exploratory synthesis of new silicates and manganese oxide with novel crystal structures and unusual oxidation states by high-temperature, high-pressure hydrothermal and flux-grow reactions.[29, 30]

In this study, single crystals of $GdNbO_4:Ln^{3+}$ (Ln = Dy, Eu) were synthesized from the HTHP hydrothermal process at 400~650 ºC in silver ampule. The luminescent property of these crystals was also investigated in detail. The $GdNbO_4$: $0.05Dy^{3+}$ single crystals showed bright white emission under different excitation wavelengths with a relatively high quantum yield of 21.7%. The $GdNbO_4$: $0.05Eu^{3+}$ exhibited excellent bright red luminescence at 612 nm under near-UV excitation, narrowed emission spectra, room temperature luminescence lifetimes of milliseconds and maximum quantum efficiencies of 43.2%, which may have potential application in optoelectronic devices.

Experimental Section

2.1. Materials and synthesis

Starting materials were Gd_2O_3, Dy_2O_3, Eu_2O_3, Nb_2O_5 (99.99%, Aldrich), KOH, NaOH (99.5%) and Nb_2O_5 (99.9%, Beijing Chemical Reagent Company). Gd_2O_3, Eu_2O_3 and Dy_2O_3 were preheated at 900 ºC overnight.

Typical synthesis procedures are the following: Gd_2O_3, Dy_2O_3, Eu_2O_3, Nb_2O_5 (1 mmol) and KOH/NaOH (2 g each, 1:1 w/w) were mixed and ground, then a small amount of water was added to make the powders homogeneously. The obtained mixture was encapsulated in a silver ampule and putted into a hydrothermal system (Model HR-1B-2, LECO Tem-Pres), as showed in Figure S1. The hydrothermal reactions were carried out under autogenous pressure of water.

The reaction was carried out at 450 ~ 650 ºC for 60 h severally while pressure of the reaction was fixed at 110 MPa. Then the product was taken out from the ampule after being cooled naturally. The resulting white flake crystals were purified and dried at 60 ºC for 2 h under vacuum after removal of the flux with ethanol. Thus, $GdNbO_4:Dy^{3+}$ and $GdNbO_4:Eu^{3+}$ single crystals were synthesized.

2.2. Measurements and characterization

A suitable crystal of product (0.10 mm × 0.05 mm × 0.03 mm) was selected for analysis on a Bruker SMART APEX 2 microfocused diffractometer using graphite-monochromated Mo Kα radiation (λ=0.071073 nm) with 50 kV and 0.6 mA at 296(2) K. Data processing was accomplished with the APEX 2. The structure of $GdNbO_4:Ln^{3+}$ was resolved by the direct method and refined by the full-matrix least-squares technique with SHELXL97. Raman spectra of I, which was excited at 532 nm, were obtained on a Renishaw *via* Confocal Raman spectrometer. The 532 nm solid state laser radiation was used as the exciting source with the power of 150 mW. Data acquisition with a 10 s accumulation was done for the detection. XPS were taken on an ESCALAB 250 electron energy spectrometer with Mg Kα (12530.6 eV) as the X-ray excitation source. The photoluminescence (PL) spectra were obtained on a FlouroMax-4 spectrophotometer with Xe 900 (150 W xenon arc lamp) as the light source. To eliminate the second-order emission from the source radiation, a cut-off filter was used during the measurement. The PL decay curves were measured on an FLS920 spectrophotometer (Edinburgh Instruments) with a μF920H flash lamp as the light source. Slit widths were 0.20 (excitation) and 0.20 (emission) nm. All spectra were recorded at room temperature.

3. Results and discussion

3.1. Phase identification of $GdNbO_4:Ln^{3+}$ (Ln = Dy, Eu) Single Crystals

The crystallization behavior and morphology of the studied samples were investigated representatively by applying XRD, FE-SEM, Raman and XPS on the $GdNbO_4:Ln^{3+}$ (Ln = Dy, Eu) single crystals. Fig. 1 shows XRD patterns of single crystals from the hydrothermal method at 450 ºC, 500 ºC, 550 ºC and 650 ºC within 60 h. As shown in Fig. 1, the product prepared at 450 ºC (Fig. 1a) was mainly Nb_2O_5, and the main phase of the product was $GdNbO_4$ with a small amount of $NaNbO_3$ at the temperature from 500 ºC to 550 ºC (Fig. 1b-c). Then the phase composition of product had no obvious changes when the temperature was increased from 550 ºC to 650 ºC. As shown in Fig. 1d, single crystals could be successfully obtained at a hydrothermal temperature of 650 ºC or above. And the temperature of 650 ºC was needed to synthesize the $GdNbO_4:Ln^{3+}$ (Ln^{3+} = Dy^{3+}, Eu^{3+}) single crystals through the high pressure hydrothermal method. Thus, the $GdNbO_4:Ln^{3+}$ single crystals could be obtained by the flux molten in this study at a temperature which was significantly lower than those in other methods.

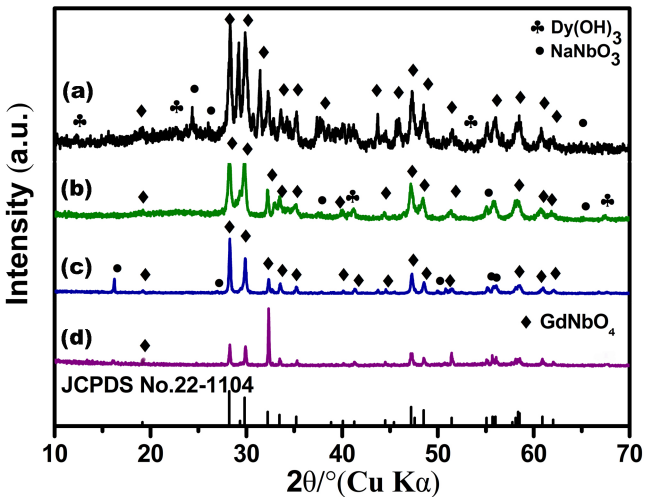

Fig.1. Power XRD patterns of the niobate solids obtained at various temperatures: (a) 450 °C , (b) 500 °C, (c) 550 °C , and (d) 650 °C for 60 h and a K : Na molar ratio of 1 : 1.

XRD patterns of the products from HP-HT hydrothermal reaction were shown in Fig. 2a. Within 2 h, the produced sample mainly contains the amorphous and crystalline phases of $GdNbO_4$:Ln^{3+}. After 24 h, pure crystalline of $GdNbO_4$:Ln^{3+} could be obtained and the corresponding XRD pattern was illustrated in Fig. 2b. With the prolonged reaction time, crystalline of the sample could be increased. As shown in Fig. 2c, the diffraction peaks could be indexed to the pure phase of $GdNbO_4$ (JCPDS: 22-1104; monoclinic phase; space group: C2/c). The narrow peaks of XRD patterns indicated that the sample was crystallized well, which was beneficial for luminescence. When the reaction time was extended to 96 h, the preferred orientation of (040) becomes more obvious.

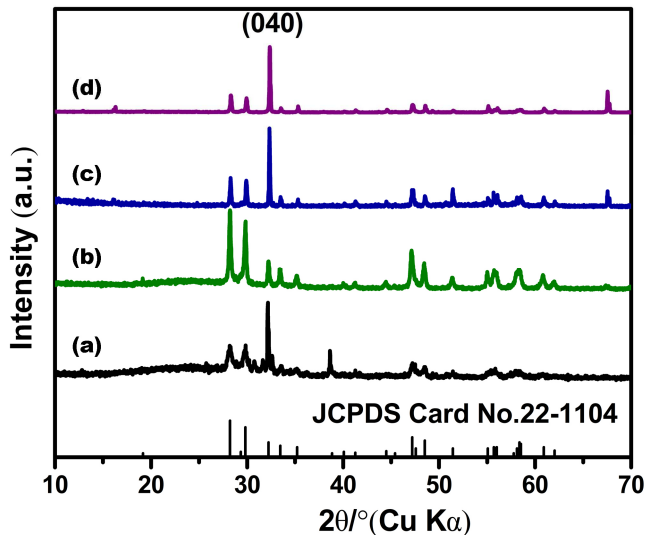

Fig.2. Power XRD patterns of the niobate solids obtained at various time: (a) 2 h, (b) 24 h, (c) 60 h, and (d) 96 h for 650 °C and a K : Na molar ratio of 1 : 1.

SEM images of the obtained samples from various hydrothermal temperatures within 60 h were shown in Fig. 3. It could be seen that the morphology remarkably was depended on the reaction temperature. At 450 ºC, Nb_2O_5 and OH^--generated short bar-like particles with a size of 10 μm (Fig. 3a). Interestingly, the niobate crystal could be assembled into sheet-like spiky balls with a size of 50~100 μm at 500 ºC (Fig. 3b). When the temperature was increased to 600 ºC, niobate crystal with high purity was produced (Fig. 3c). Larger sheets could be synthesized at higher hydrothermal temperatures (Fig. 3d). At 650 ºC, the proportion of the sheet in the product was increased during the reaction until all the products were sheet. Clearly, the niobate products with the desired morphology could be tailored through the careful control on the holding temperature.

The reaction time-dependent morphological evolution was investigated with SEM (see Fig. 4). The microcrystal was reunited together like amorphous forms within 2 h as showed in Fig.4a. And many $GdNbO_4$:Ln^{3+} single crystals could be formed within 24 h (Fig. 4b). After 24 h, the form of 50 –100 μm sheets in tens of micrometres of length and nanometer of width was formed (Fig. 4c). With the further extension of reaction time to 60 h, $GdNbO_4$:Ln^{3+} single crystals were formed (Fig. 4d). Therefore, the metastable phase was time-dependent and only formed within a very narrow temperature range.

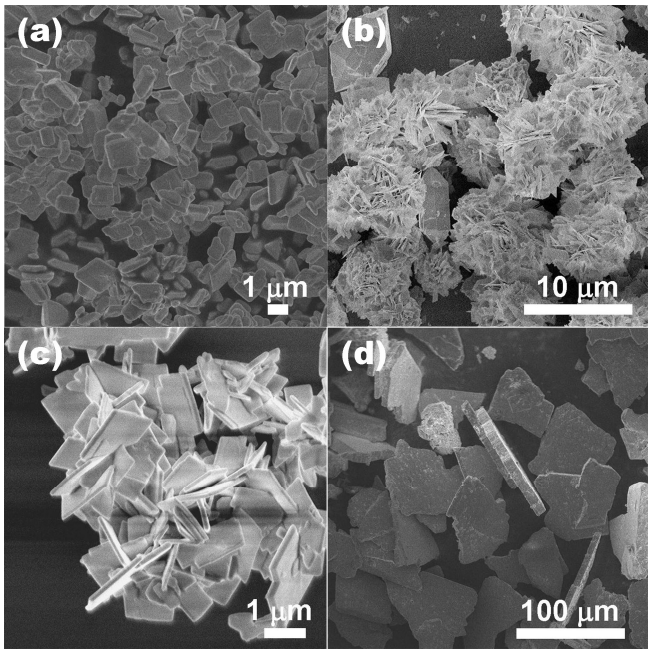

Fig.3. SEM images of the niobate solids obtained at various temperatures: (a) 450 °C , (b) 500 °C , (c) 550 °C and (d) 650 °C for 60 h and a K : Na molar ratio of 1 : 1.

As reported previously, niobates nanostructures were synthesized in solution *via* a dissolution-precipitation process. Nb_2O_5 was dissolved into $Nb_6O_{19}^{8-}$ ions to form single octahedron NbO_6^{7-} anions via complex transforms[31]. Similarly, the equation could be applied to $GdNbO_4$ single crystals as the following:

$$3Nb_2O_5 + 8OH^- \rightarrow Nb_6O_{19}^{8-} + 4H_2O \quad (1)$$

$$Nb_6O_{19}^{8-} + 34OH^- \rightarrow 6NbO_6^{7-} + 17H_2O \quad (2)$$

$$NbO_6^{7-} + (1-x)K^+ + xNa^+ + 3H_2O \rightarrow K_{1-x}Na_xNbO_3 + 6OH^- \quad (3)$$

$$K_{1-x}Na_xNbO_3 + Ln^{3+} + 2OH^- \rightarrow LnNbO_4 + (1-x)K^+ + xNa^+ + H_2O \quad (4)$$

As described in Step (1), the Nb_2O_5 was dissolved simultaneously in the $Nb_6O_{19}^{8-}$ ions at the initial stage of the hydrothermal reaction. As showed in Fig. S2a, Then single octahedron NbO_6^{7-} anions were formed by complex transforms under lower alkaline conditions after Step (2). In Step (3), the tiny crystalline nucleation in a supersaturated medium was formed and followed by the crystal growth of $K_{1-x}Na_xNbO_3$ (KNN) under hydrothermal conditions (Fig. S2b). The formation process of the niobates structure was illustrated in equation. The reaction could be done simultaneously during the crystalline nucleation due to the high super saturation of medium at the initial stage, which promoted the continuous growth of $LnNbO_4$ crystals to form several crystalline nuclei

(Fig. S2c). Then the grains grew larger and larger step by step, and the grains close each other might merge together to formed a larger structure that consisted of a number of interlacing micro-crystals (Fig. S2d). As the reaction continued, the close micro-crystals with the same orientation could also gradually merge together due to the aggregation growth during the hydrothermal reaction, thus to form step-like sheets as shown in Fig. S2e. The single crystals $Gd(OH)_3$ were formed under higher alkaline conditions as showed in Fig. S2f. Crystal data are given in Table S1: hexagonal, a = 0.6350 (12) Å, b = 0.6350 (12) Å, c = 0.3642 (15) Å. Therefore, the as-prepared $LnNbO_4$ should be resulted from the octahedron crystal structure of NbO_6^{7-} anions and the oriented attachment via the aggregation growth mechanism.

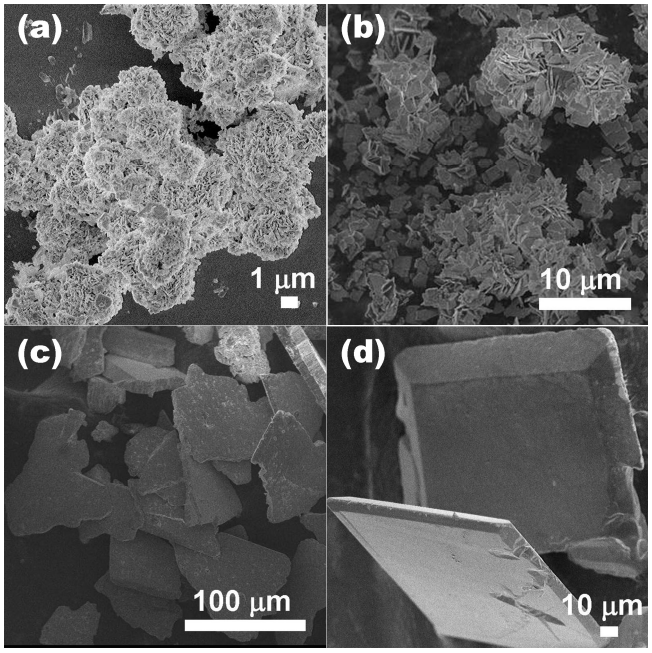

Fig.4. SEM images of the niobate solids obtained at various time: (a) 2 h, (b) 24 h, (c) 60 h, and (d) 96 h at 650 °C and a K : Na molar ratio of 1 : 1

Structure of the Dy^{3+}, Eu^{3+}-doped $GdNbO_4$ single crystal was identified with powder XRD as shown in Fig. S3(a-b). The typical XRD pattern of the single crystal indicated that the sample is highly crystalline. Crystal data are given in Table S2: monoclinic, space group *C*2/*c*, a = 7.160(5) Å, b = 11.170(10) Å, c = 5.139(4) Å, β = 131.156(10)º, V = 309.5(4) $Å^3$ and *Z* = 4. Compared the results with the JPCDS data, it was confirms the validity of the experimental data, which is consistent with the data from the MDI jade 5.0 analysis software. It is worth noting that the reaction temperature must be carefully optimized to yield high purity products with the desired single crystal. It was also found that, with increasing reaction temperature, the thermal active energy promoted the transformation of intermediates to generate the final products.

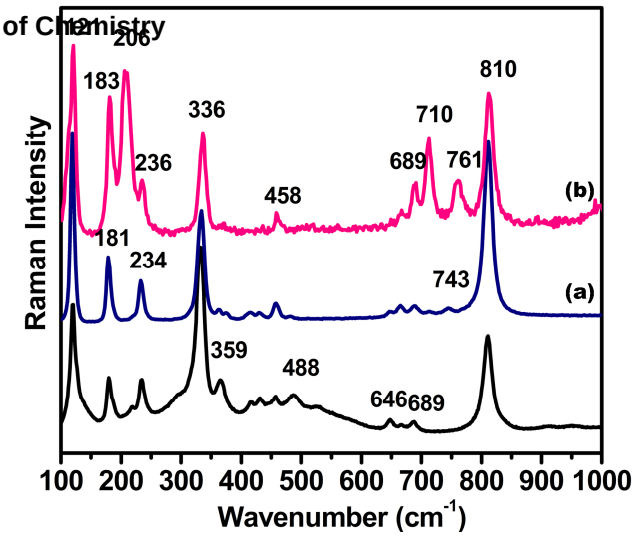

Fig.5. (a) Raman spectrum of the as-synthesized Dy^{3+} doped $GdNbO_4$. (b) Raman spectrum of the as-synthesized Eu^{3+} doped $GdNbO_4$.

The EDS results confirm the presence of oxygen (O), niobium (Nb), Gadolinium (Gd) and Dysprosium (Dy) elements in the $Gd_{1-x}Dy_xNbO_4$ sample (Fig. S4a), and oxygen (O), niobium (Nb), Gadolinium (Gd), and Europium (Eu) elements in $Gd_{1-x}Eu_xNbO_4$ sample (Fig. S4b), respectively.

As showed in Fig. 5. We compared Raman spectra of $GdNbO_4$, (a) $Gd_{1-x}NbO_4$:Dy_x (x = 0.05), (b) $Gd_{1-x}NbO_4$:Eu_x (x = 0.05). The relative strengthening of the bands around 128, 189, 220, 317, 337, 362, 417, 433, 649 and 688 cm^{-1} was accompanied by the relative weakening of bands at 122, 124, 181, 235, 331, 459, 667 and 812 cm^{-1}, which indicated that these Raman-active modes were belonged to the Bg and Ag symmetries, respectively.[2] We observed ν_1, ν_2, ν_3 and ν_4 vibration modes from the host lattice $GdNbO_4$, which correspond to a regular NbO_4 tetrahedron with no interactions and distortions at 812(ν_1), 649(ν_3), 417(ν_4), and 337cm^{-1}(ν_2) predicated. Raman bands appearing at 812 and 337 cm^{-1} are due to Nb-O symmetric modes of the NbO_4 tetrahedral structure, and Raman bands appearing at 649 and 417 cm^{-1} are due to Nb-O anti-symmetric modes of the NbO_4 tetrahedral structure.

The phonon energies below 300 cm^{-1} are assigned to external vibrations. From Fig. 5 one can see that all doped samples have the same monoclinic M-phase as $GdNbO_4$ with no interactions and distortions at 812, 649, 417 and 337 cm^{-1}. It means that no considerable changes in the crystalline structure are observed. The Raman spectra of $GdNbO_4$: Eu, Dy (Fig. 5a-b) single crystals was significantly different from that of the pure $GdNbO_4$ crystals, which confirmed that Eu^{3+} or Dy^{3+} ions effectively entered the lattice of host ($GdNbO_4$) through replacing Gd^{3+} ions. Four new peaks in the Raman spectroscopy around 458, 503, 689, 710 and 761 cm^{-1} in all doped samples (Fig. 6a-b) appeared and we assume that they are related to Ln^{3+} activation because their shape and position correspond to luminescence spectra. At room temperature, He-Ne laser (632.8) can excite Eu^{3+} ions to $^5D_0$ energy level. The

luminescence from $^5D_0$ energy level to $^7F_3$ band gets to 650-660 wavelength regions.

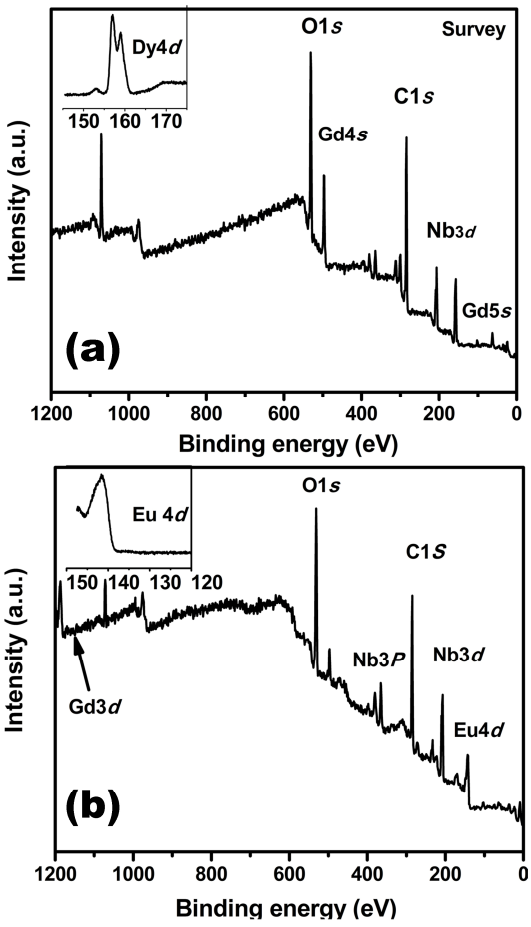

Fig.6. XPS spectra of $GdNbO_4$:Dy^{3+}, Eu^{3+} single crystal synthesized at 650 ºC for 60 h. Insets are the corresponding binding energy data for Dy^{3+} and Eu^{3+}.

Surface composition of the as-synthesized $GdNbO_4$:Dy^{3+} single crystals were further analyzed with XPS as shown in Fig.6a. The binding energy data (calibrated using C (1s, 284.7 *eV*) as the reference) from $GdNbO_4$:Dy^{3+} was well consistent with the previous reported data of niobates. the peaks at about 530, 206, 208 and 141 *eV* were the binding energies of O (1*s*), Nb (3*d*) and Gd (4*d*), respectively.[32-34] Additionally, the binding energy of Dy (4d, 169.1 *eV*) could also be detected, which was presented in detail (inset in the picture). With the previous EDS analysis, it could be deduced that these signals could be attributed to the corresponding $GdNbO_4$:Dy^{3+} as shown in Fig. 6b with the clear bonding energy of Eu ($3d_{5/2}$, 1134 *eV*).

3.2. Photoluminescence properties

The PL excitation spectrum of the $GdNbO_4$ host lattice was shown in Fig. S5a. The broad band at 264 nm was attributed to the 2P(O)-4d(Nb) charge-transfer and a weak absorbed by the NbO_4 groups in $GdNbO_4$ is transferred to the Gd^{3+} ions. As showed in Fig. S5b, the emission spectrum consisted of a broad emission band in the 300~500 nm range with a maximum at 446 nm. Others reported this band was at 445 nm.[35] Although the $LaNbO_4$:Eu^{3+}, Tb^{3+} with a fergusonite structure was reported as a promising phosphor for solid state lighting,[37] white light from $GdNbO_4$:Dy^{3+} single crystal had not been reported yet except the significant host emission in its emission spectrum.

The excitation spectrum of Dy^{3+}-doped $GdNbO_4$ (λ_{em} = 576 nm) as showed in Fig.7a, consists of a broad band centered at around 270 nm, which is attributed to the host absorption. The presence of host absorption when Dy^{3+} emission is monitored indicates host to activator energy transfer. The O^{2-}-Dy^{3+} charge transfer band located below 200 nm.[38] The dominant band was observed at 352 nm, which corresponds to the $^6H_{15/2} \rightarrow {}^6P_{7/2}$ transition of Dy^{3+}. The emission spectrum of Dy^{3+} doped $GdNbO_4$ under host excitation (270 nm) (Fig. 7b) consists of two strong bands at 492 nm and 576 nm corresponding to the characteristic $^4F_{9/2} \rightarrow {}^6H_{15/2}$ and $^4F_{9/2} \rightarrow {}^6H_{13/2}$ transitions of Dy^{3+}, respectively. The $^4F_{9/2} \rightarrow {}^6H_{11/2}$ emission band was too weak to be observed. In addition, a moderately intense broad emission band centered at around 446 nm was observed, which corresponded to the NbO_4^{3-} moiety of the host.[39]

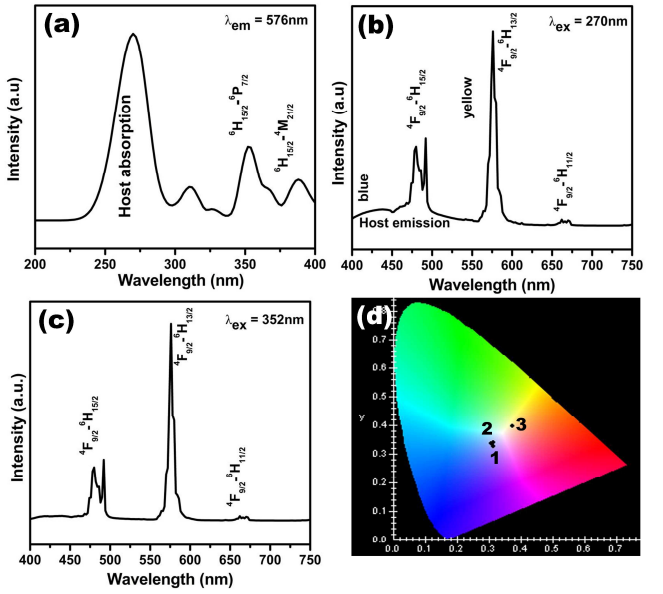

Fig.7. Room-temperature excitation of $GdNbO_4$:Dy^{3+} (a), Emission spectra of $GdNbO_4$:Dy^{3+} under 270 nm (b), Emission spectra of $GdNbO_4$:Dy^{3+} under 352 nm external lamp (c), CIE chromaticity diagram of $GdNbO_4$:Dy^{3+} single crystal with different excitation wavelength (the point 1~3 are corresponding to the λ ex = 270, 352 and 388 nm, respectively), (d).

The presence of an emission of the host indicated that the energy transfer from the host to Dy^{3+} was incomplete. If the host transfers the absorbed energy completely to Dy^{3+}, the emission bands of Dy^{3+} should only be observed as that in the $Na_2Sr(PO_4)F$:Dy^{3+} system.[40] The presence of a host emission band was useful to generate white light. This was also illustrated in some examples such as Dy^{3+}, Tm^{3+} and Eu^{3+} co-activated $KSr_4(BO_3)_3$,[41] in which the white light emission came from the combination of the host emission band and the Dy^{3+}

emission band due to the host-to-Dy^{3+} energy transfer. The emission spectrum of Dy^{3+}-doped $GdNbO_4$ at 352 nm excitation as shown in Fig. 7c has two strong bands at 492 nm and 576 nm, due to the characteristic $^4F_{9/2} \rightarrow {}^6H_{15/2}$ and $^4F_{9/2} \rightarrow {}^6H_{13/2}$ transitions of Dy^{3+}, respectively.

The emission appeared yellow to the naked eye at 352 nm of excitation. However, when checked in a spectrophotometer, some of the Dy^{3+}-doped host lattices emitted white light at suitable yellow-to-blue intensity ratio. The emission was overlapped by several red lines at 492, 576 and 675 nm. Emission bands were observed at 492 nm and 576 nm due to the $^4F_{9/2} \rightarrow {}^6H_{15/2}$ (magnetic dipole) and the $^4F_{9/2} \rightarrow {}^6H_{13/2}$ (electric dipole) transitions of Dy^{3+}, respectively. The $^4F_{9/2} \rightarrow {}^6H_{11/2}$ emission band is too weak to be observed. A weak broad band is observed at 446 nm due to the host emission. Electric dipole transition is dominant only when the Dy^{3+} ions occupy sites with no inversion centers. Dy^{3+} emits white light in most of the host lattices at a suitable yellow-to-blue which in turn depends on the site symmetry and the concentration of Dy^{3+}. In contrast, the compound emitted yellow light under 352 nm of excitation when the host emission in the blue region was absent. [42]

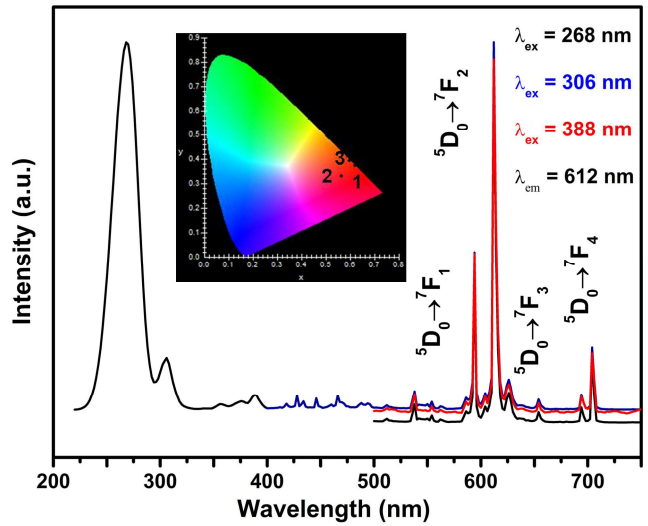

Fig.8. Room-temperature excitation of $GdNbO_4$:Eu^{3+}, Emission spectra of $GdNbO_4$:Eu^{3+} under 268 nm, 306 nm and 388 nm, respectively. Inset is CIE chromaticity diagram of $GdNbO_4$:Eu^{3+} single crystal with different excitation wavelength (the point 1~3 are corresponding to the λ_{ex} = 268, 306 and 388, respectively).

The luminescence color was changed from nearly white to yellow as shown in Fig.7d. Nearly white light was achieved at λ_{ex} = 270, 388 and 352 nm and the CIE values were (0.3135, 0.3421), (0.3088, 0.3380) and (0.3146, 0.3296) respectively, which were close to the ideal white light (0.33, 0.33). Furthermore, when the wavelength was changed to 270 nm, the quantum yield of the material was ~21.7%. It was well known that the energy level difference between ^6G_J and ^6P_J of Gd^{3+} was close to that between $^7F_1$ and $^5D_0$ of Eu^{3+}, and Gd^{3+} in ^6G_J state could excite Eu^{3+} into $^5D_0$ state by resonance energy transfer to in the energy transfer of Gd^{3+} to Eu^{3+}. The energy transfer process in $GdNbO_4$:Eu^{3+} might be described as the following. The energy excited the excitation source NbO_4^{3+}, and the energy was trapped by Gd^{3+} and migrated along them until it was trapped by Eu^{3+}. Then the characteristic luminescence was resulted. Additionally, the NbO_4^{3+} could transfer the energy to activators directly.[43]

Fig.8 showed the excitation and emission spectrum of $GdNbO_4$:Eu^{3+} with the different excitation wavelengths. The typical lines of the Eu^{3+} ions centering at 536, 558, 591, 612, 646 and 695 nm, which can be ascribed to the $^5D_1 \rightarrow {}^7F_1$ and $^5D_0 \rightarrow {}^7F_J$ (J = 0,1,2,3,4), respectively. Beside, the crystal field splitting of the $^5D_0 \rightarrow {}^7F_{1,2,4}$ transitions is visible, indicating the good crystalline of the samples. No emission from the NbO_4^{3-} ions can be detected, revealing the high efficient nonradiative energy transfer from the NbO_4^{3-} ions to the Eu^{3+} ions. In $GdNbO_4$:Eu^{3+} crystal structure, the doped Eu^{3+} ion will occupy the site of the Gd^{3+} ion, where the Gd^{3+} bond to four vertices of NbO_4 tetrahedron with Nb-O = 2.146 Å and two edges of NbO_4 tetrahedron Gd-O = 1.1916 Å, forming a GdO_8 distorted triangulate dodecahedron, as illustrated in Fig. S2.

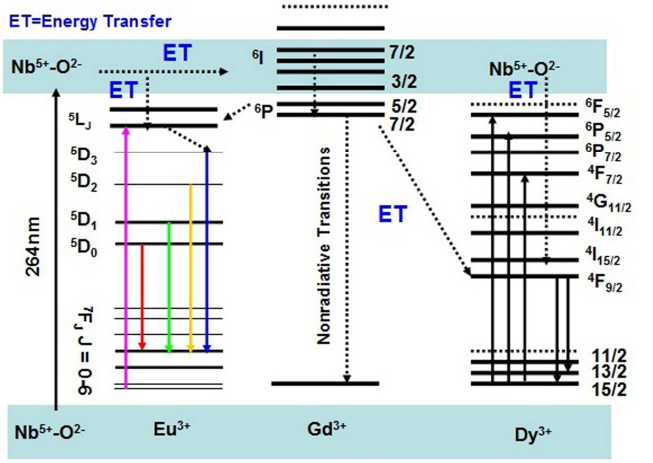

Fig.9. A simple model illustrating the energy transfer from $O^{2-} \rightarrow Nb^{5+}$ charge transfer band to Gd^{3+}, Eu^{3+} and Dy^{3+} ions, the concentration quenching of Gd^{3+}, and the characteristic emission of Eu^{3+} and Dy^{3+} ions in $GdNbO_4$.

The dodecahedron can be visualized to give Gd^{3+} ions *D2d* point group which has very low inversion symmetry. Generally, when Eu^{3+} occupies a site with inversion symmetry, the $^5D_0 \rightarrow {}^7F_1$ magnetic dipole transition will be dominant, while the $^5D_0 \rightarrow {}^7F_2$ forced electric dipole transition will take the dominant role if Eu^{3+} occupies a site without inversion symmetry. Here, the high intensity ratio of 612 nm ($^5D_0 \rightarrow {}^7F_2$) to 591 nm ($^5D_0 \rightarrow {}^7F_1$) peaks is consistent with the above analysis. The emission from higher energy was attributed to the low energy vibration of NbO_4^{3-} groups. The multi-phonon relaxation by NbO_4^{3-} was not able to bridge the gaps between the higher energy levels ($^5D_1$, $^5D_2$ and $^5D_3$) and the $^5D_0$ level of Eu^{3+} completely, which resulted in emissions from these higher levels.[44-47]

A simple model illustrating the energy transfer from the NbO_4 ($O^{2-} \rightarrow Nb^{5+}$ charge transfer band) group to the Gd^{3+} ion,

concentration quenching of the Gd^{3+} ion, and the energy transfer from the $O^{2-} \rightarrow Nb^{5+}$ charge transfer band to Eu^{3+} and Dy^{3+} ions process in $GdNbO_4$ is shown in Fig.9. $GdNbO_4$ is insert to UV due to the fact that all excitation energy is transferred from the NbO_4 group ($O^{2-} \rightarrow Nb^{5+}$ charge transfer band) to the Gd^{3+} ion and subsequently concentration quenching of Gd^{3+} ion. When doping with Eu^{3+} or Dy^{3+} ions in $GdNbO_4$, situations completely change. In $GdNbO_4$:Eu^{3+}, Dy^{3+}, the NbO_4 group absorbs UV efficiently and transfers its energy to Gd^{3+} ion; the energy migrates over the Gd^{3+} sub-lattice until it is trapped by Eu^{3+} or Dy^{3+} ion and gives its characteristic red (white) emission. Besides this, due to energy level match, the NbO_4 group ($O^{2-} \rightarrow Nb^{5+}$ charge transfer band) can also transfer the excitation energy to Eu^{3+} or Dy^{3+} ion activators directly, resulting in the characteristic emission of Eu^{3+} or Dy^{3+}.[48]

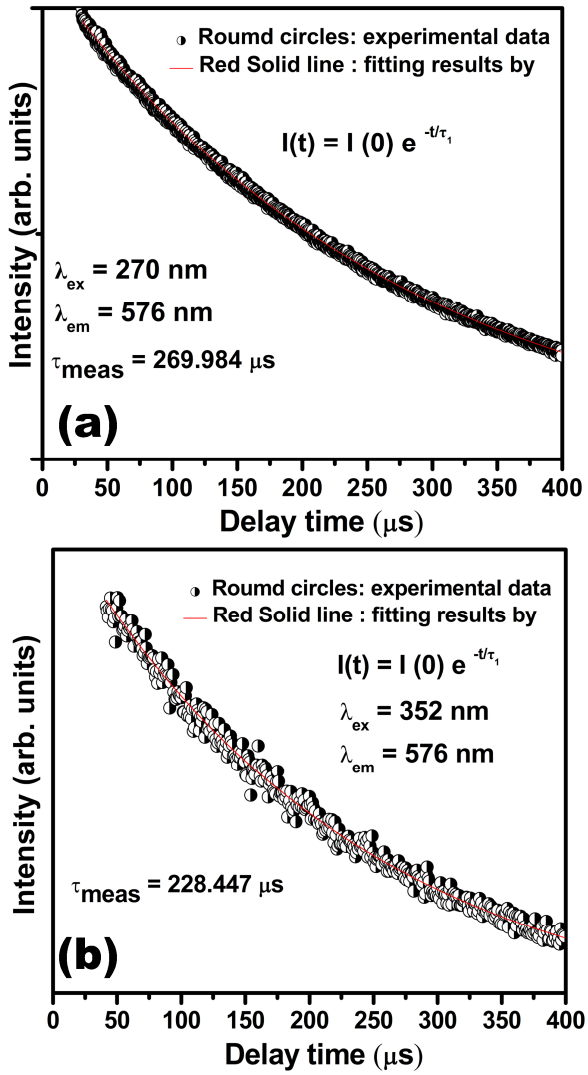

Fig.10. (a) Luminescence decay time of $GdNbO_4$:Dy^{3+} (5%), λ_{ex} = 270 nm ;(b) λ_{ex} = 352 nm

In summary, $GdNbO_4$ was an appropriate host for Dy^{3+} ion. The presented emission spectra showed intense emission bands under UV radiation, which could be assigned to the f-f transitions of Dy^{3+} ions. Furthermore, the measured decay time of the excited state of $^4F_{9/2}$ was 269.84 μs for 5% Dy^{3+}-doped $GdNbO_4$ single crystal phosphors and the decay was also found to be a single exponential under 270 nm excitation as shown in Fig.10a, which was typical characteristic of Dy^{3+} in inorganic matrices. [49]

The characteristics of the excitation spectra, the observed emission and the luminescence decay times all were due to the energy transfer (ET) from the charge transfer (CT) state of the matrix to the Dy^{3+} ion. The absence of the luminescence peaks, which were higher than $^1G_4$, $^4F_{9/2}$ and $^5D_2$ for the transitions of the Dy^{3+} ion, suggested that the ET occurred at the Dy^{3+} level. Although this ET was slightly lower than the CT state of $GdNbO_4$, the energy gap between them was large enough to eliminate the reverse ET. The measured decay time of the excited state of $^4F_{9/2}$ was 228.467 μs for Dy^{3+}-doped $GdNbO_4$ single crystal phosphors and the decay was found to be a single exponential under 352 nm excitation as shown in Fig.10b, which was also typical for Dy^{3+} in inorganic matrices.[50-52]

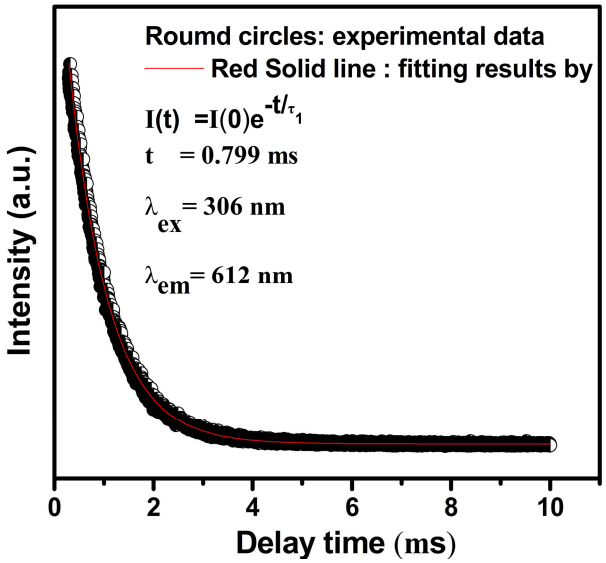

Fig.11. Luminescence decay times of $GdNbO_4$:Eu^{3+} (5%), λ_{ex} = 306 nm

In addition, the NbO_6 polyhedral share edges with the GdO_8 polyhedral. The GdO_8 polyhedral share edges with each other to form zig-zig chains along the c-direction (Fig.S6). The chains are in turn connected through an edge-sharing GdO_8 polyhedron to form a 3-D network. As a result, the 1-D zig-zig chains of the NbO_6 polyhedral are isolated from each other, whereas the GdO_8 polyhedral are interconnected in all three crystallographic directions. The Nb–O–Nb and Nb–Gd–Nb bond angles are 104.2° and 170.779°, respectively. Hence, the energy transfer from the host to the activator ion will not be facile, whereas the rapid migration of energy between the activator ions located on the Gd^{3+} sites would be facilitated.

Hence, the chromaticity for this sample is improved, and the colour is redder instead of common orange-red emission characteristic of niobates. This agrees with the Eu^{3+} ion

environment and structure of single crystal that favours placing the Eu^{3+} ions on lattice, where the local symmetry is highly distorted. It is noticed that the intensive emission of the electronic dipole transition at 612 nm is narrow. The emission peak at 612 nm is relatively stronger than that at 591 nm, which is beneficial for obtaining a phosphor with good color purity. It is known that the $^5D_0$ - $^7F_2$ electric dipole transition of Eu^{3+} is highly sensitive to its local environment, which appears dominantly only when the Eu^{3+} ion is in a low symmetry site. The $^5D_0$-$^7F_1$ line was observed at 591 nm, which originates from the parity-allowed magnetic dipole transition and is insensitive to the crystal field environment[53]. As a result, in the site with an inversion symmetry, the magnetic dipole transition of $^5D_0$ - $^7F_1$ is dominant, whereas in the site without inversion symmetry, the electronic transition of $^5D_0$ - $^7F_2$ becomes dominant[54].

Fig.11 showed the room temperature luminescence decay curves of $^5D_0$ - $^7F_2$ (612 nm) for $Gd_{1-x}Eu_xNbO_4$ (x = 0.05) under 306 nm excitation. The luminescence decay curves of the $^5D_0$ level of the samples can be well simulated by a single-exponential function, $I = A \exp(-t/\tau) + y_0$, where τ is the luminescent lifetime, and A is the fitting parameter. The lifetimes for the $^5D_0$ - $^7F_2$ transitions of Eu^{3+} were calculated to be t = 0.799 ms for $Gd_{1-x}Eu_xNbO_4$ (x = 0.05). The single decay time indicates that the chemical environment of the Eu^{3+} ions is uniform.[55, 56] The luminescence lifetime is the longest for 5% doped materials and then shortens slightly with increasing dopant concentration in the $Gd_{1-x}Eu_xNbO_4$ host. The reducing of the emission effective lifetimes can be connected with cross-relaxation between the Eu^{3+}. The quantum efficiencies (η) measured are 43.2 for $Gd_{1-x}NbO_4$:Eu_x (x = 0.05).

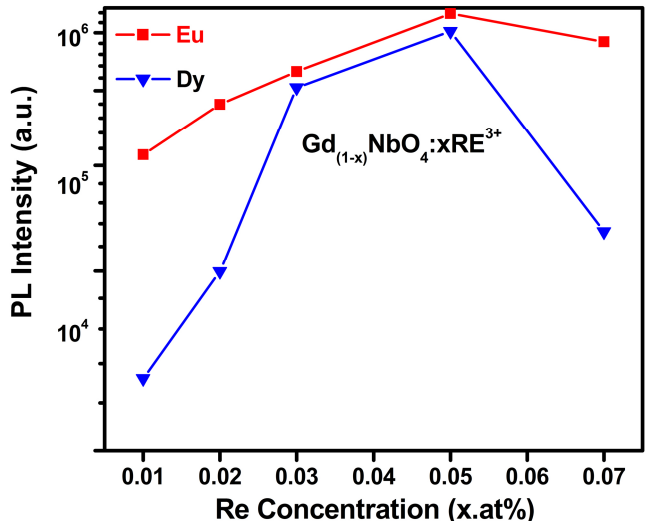

Fig.12. The PL intensity of Eu^{3+} and Dy^{3+} ions as a function of their doping concentration (x) in $Gd_{(1-x)}NbO_4$:xEu^{3+} and $Gd_{(1-x)}NbO_4$:xDy^{3+}.

By varying the contents of Eu^{3+} and Dy^{3+} ions in $GdNbO_4$, we determined the compositions with the highest emission intensity. Fig.12 shows the PL intensity of Eu^{3+} and Dy^{3+} as a function of their doping concentration (x) in $Gd_{1-x}NbO_4$:xEu^{3+} (red dots) and $Gd_{1-x}NbO_4$:xDy^{3+} samples (blue dots), respectively. It can be found that the PL emission intensity of Eu^{3+} increases with the increase of its concentration (x) first, reaching a maximum value at x = 0.05, and then decreases with increasing concentration (x) due to the quenching effect. Thus, the optimum concentration of Eu^{3+} is determined to be 5 at% of Gd^{3+} in the $GdNbO_4$ host lattice.

In general, the concentrations quenching of luminescence is due to the energy migration among the activator ions at the high concentrations. In the energy migration process, the excitation energy will be lost at a killer or quenching site, resulting in the decrease of PL intensity. For the concentration quenching of Dy^{3+} in $Gd_{1-x}NbO_4$:Dy^{3+} samples, luminescence is mainly caused by cross relaxation; energy transfers from one Dy^{3+} to another that matches in energy. These transitions are mainly Dy^{3+} ($^4F_{9/2}$, $^6H_{15/2}$) → Dy^{3+} ($^6F_{3/2}$, $^6F_{11/2}$). The optimum concentration for Dy^{3+} is 0.05 of Gd^{3+} in the $GdNbO_4$ host lattice.[57]

Conclusions

Dy^{3+}, Eu^{3+}-doped $GdNbO_4$ single crystals were synthesized via a hydrothermal method under high temperature high pressure conditions. High temperature (650 ºC) was found to be favorable for the growth of orthoniobate single crystals. When phosphors were excited with near-UV light, the doped Ln ions exhibited their characteristic emission in the $GdNbO_4$ host lattice because of the efficient energy transfer from the [NbO_4] groups. The PL properties of ternary niobates under UV light excitation were studied. Dy^{3+}- doped $GdNbO_4$ exhibited intensive white light under host excitation. The emission transition from the relatively high level $^5D_1$, $^5D_2$ and $^5D_3$ of all Eu^{3+}, phosphors was observed possibly because of the low probability of multi-phonon relaxation between the Eu^{3+} ions in $GdNbO_4$ hosts. The results indicated that Ln^{3+}-doped $GdNbO_4$ is a very promising material for optoelectronics and solid-state lighting of general illumination.

Acknowledgements

This work was supported by the National Sciences Foundation of China (No.21271082, 21371068).

Notes and references

a State Key Laboratory of Inorganic Synthesis and Preparative Chemistry Jilin University. 2699 Qianjin Street, Changchun.
b School of Chemistry & Chemical Engineering, Anqing Normal University, Anqing, Anhui 246011, China.
[c] Address here.

1. E. S. Octaviano, D. R. Ardila, L. H. C. Andrade, M. S. Li and J. P. Andreeta, *Cryst Res Technol* ., 2004, 39, 859.
2. K. P. F. Siqueira, R. L. Moreira and A. Dias, *Chem. Mater.*, 2010, 22, 2668.
3. L. An, A. Ito and T. Goto, *Ceram Int.*, 2013, 39, 383.
4. S. Tachi, K.I. Kakimoto and I. Kagomiya, *Ceramics International*, 2012, 38, 311.
5. Z. Bi, J. P. Martínez, J. H. Kim, C. A. Bridges, A. Huq, J. P. Hodges and M. P. Paranthaman, *Int. J. Hydrogen Energy.*, 2012, 37, 12751.

6. S. A. Naidu, S. Boudin, U. V. Varadaraju and B. Raveau, *J. Mater. Chem.,* 2012, 22, 1088.
7. N. Guo, Y. Zheng, Y. Jia, H. Qiao and H. You, *New J Chem.*, 2012, 36, 168.
8. R. Singh and S. J. Dhoble, *Luminescence.*, 2011, 26, 728.
9. A. Kudo, Kato, Hideki,Nakagawa, Seira, *J. Phy. Chem. B.*, 1999, 104, 571.
10. P. Huang, C. Qin. Z. M. Su, Y. Xing, X. L. Wang, K. Z. Shao, Y. Q. Lan, and E. B. Wang, *J. Am. Chem. Soc.*, 2012, 134, 14004.
11. Z. Y. Zhang, Q. P. Lin, D. Kurunthu, T. Wu, F. Zuo, S. T. Zheng, C. J. Bardeen, X. H. Bu and P. Y. Feng, *J. Am. Chem. Soc.*, 2011, 133, 6934.
12. A. L. Viet, M. V. Reddy, R. Jose, B. V. R. Chowdari and S. Ramakrishna, *J. Appl. Phys.*, 2010, 24, 664.
13. Y. Kobayashi, M. L. Tian, M. Eguchi and T. E. Mallouk, *J. Am. Chem. Soc.*, 2009 131, 9849.
14. X. Xiao and B. Yan, *J Alloy Compd.*, 2006, 421, 252.
15. G. D. Dzik, W. R. Romanowski, R. Lisiecki, P. Solarz, B. Macalik, M. Berkowski, M. Głowacki and V. Domukhovski, *Cryst Growth Des.*, 2010, 10, 3522.
16. I. P. Roof, M. D. Smith, S. Park and H. C. zur Loye, *J. Am. Chem. Soc.,* 2009, 131, 4202.
17. P. Zhang, T. Wang, W. Xia and L. Li, *J Alloy Compd.,* 2012, 535, 1.
18. V. V. Galutskiy, M. I. Vatlina and E. V. Stroganova, *J Cryst Growth*, 2009, 311, 1190.
19. I. P. Roof, T. C. Jagau, W. G. Zeier, M. D. Smith, H. C. Loye and J. K. M. Lett, *J. Appl. Phys.*, 2009, 5, 1955.
20. I. P. Roof, S. Park, T. Vogt, V. Rassolov, M. D. Smith, S. Omar, J. Nino and H. C. zur Loye, *Chem. Mater.,* 2008, 20, 3327.
21. C. H. Y. X. Lim, A. Sorkin, Q. Bao, A. Li, K. Zhang, M. Nesladek and K. P. Loh, *Nat Commun.*, 2013, 4, 1556.
22. K. Zhu, Y. Cao, X. Wang, L. Bai, J. Qiu and H. Ji, *Cryst Eng Comm*, 2012, 14, 411.
23. G. Li, L. Li, M. Li, Y. Song, H. Zou, L. Zou, X. Xu and S. Gan, *Mater Chem Phys.*, 2012, 133, 263.
24. S. Ferdov, R. A. S. Ferreira, Z. Lin and Z. Wu, *J.Solid. State. Chem.*, 2012, 190, 18.
25. H. K. Liu, W. J. Chang and K. H. Lii, *Inorg Chem.,* 2011, 50, 11773.
26. X. Guo, J. Yang, Y. Deng, H. Wei and D. Zhao, *Eur. J. Inorg. Chem.*, 2010, 22, 1736.
27. G. Demazeau, *J. Phys.: Condens. Matter.*, 2002, 14. 11031.
28. C. Y. Li, C. Y. Hsieh, H. M. Lin, H. M. Kao and K. H. Lii, *Inorg Chem.*, 2002, 41, 4206.
29. X. G. Zhao, J. Y. Li, P. Chen, Y. Li, Q. X. Chu, X.Y. Liu, J. H. Yu and R. R. Xu, *Inorg. Chem.*, 2010, 49. 9833.
30. Q. X. Chu, X. F. Wang, X. H Zhang, Q. L. Li and X. Y. Liu, *Inorg. Chem.*, 2011, 50, 2049.
31. K. J. Zhu, Y. Cao, X. H. Wang, L. Bai, J. H. Qiua and H. L. Jia, *CrystEngComm*, 2012, 14, 411.
32. V. V. Atuchin, I. E. Kalabin, V. G. Kesler and N. V. Pervukhina, *J. Electron Spectrosc.*, 2005, 142, 129.
33. J. Xu, X. H. Huang, N. L. Zhou, J. S. Zhang, J. C. Bao, T. H. Lu and C. Li, *Mater Lett.*, 2004, 58, 1938.
34. A. T. Kozakov, A. G. Kochur, A. V. Nikolsky, K. A. Googlev, V. G. Smotrakov and V. V. Eremkin, *J. Electron Spectrosc.*, 2011, 184, 508.
35. X. M. Liu and J. Lin, *J. Lumin.*, 2007, 123, 700.
36. X. Jing, C. Gibbons, D. Nicholas, J. Silver, A. Vecht and C. S. Frampton, *J Mater Chem.*, 1999, 9, 2913.
37. E. Y. Lee and Y. J. Kim, *Thin Solid Films.*, 2010, 518, 72.
38. J. Pisarska, *Opt Mater.*, 2009, 31, 1784.
39. D. F. Zhang, A. Tang, L. Yang and Z. T. Zhu, *Int. J. Min. Met. Mater.*, 2012, 19, 1036.
40. I. M. Nagpure, V. B. Pawade and S. J. Dhoble, *Luminescence : the journal of biological and chemical luminescence.*, 2010, 25, 9.
41. L. Wu, Y. Zhang, M. Gui, P. Lu, L. Zhao, S. Tian, Y. Kong and J. Xu, *J. Mater. Chem.,* 2012, 22, 6463.
42. L. Qin, D. L. Wei, Y. L. Huang, S. I. Kim, Y. M. Yu and H. J. Seo, *Inorg. Chem.*, 2013, 52, 10407.
43. T. Grzyb, A. Szczeszak, J. Rozowska, J. Legendziewicz and S. Lis, *J. Phys. Chem. C.*, 2012, 116, 3219.
44. L. Qin, Y. Huang, T. Tsuboi and H. J. Seo, *Mater Res Bull.*, 2012, 47, 4498.
45. S. H. Park, K. H. Lee, S. Unithrattil, H. S. Yoon, H. G. Jang and W. B. Im, *J. Phys. Chem. C.*, 2012, 116, 26850.
46. J. Huang, L. Zhou, X. He and F. Gong, *Chinese. J. Chem.*, 2011, 29, 441.
47. I. P. Roof, M. D. Smith, S. Park, and H. C. zur Loye, *J. Am. Chem. Soc.*, 2009, 131, 4202.
48. Y. Lü, X. H. Tang, L. S. Yan, K. X. Li, X. M. Liu, M. M. Shang, C. X. Li and J. Lin., *J. Phys. Chem. C.*, 2013, 117, 21972.
49. Y. S. Zhu, W. Xu, H. Z. Zhang, W. Wang, S. Xu and H.W. Song, *J. Phys. Chem. C.*, 2012, 116, 2297.
50. B. Tian, B. Chen, Y. Tian, J. Sun, X. Li, J. Zhang, H. Zhong, L. Cheng and R. Hua, *J. Phys. Chem. Solids.*, 2012, 158, J6.
51. M. Jayasimhadri, B. V. Ratnam, K. Jang, H. S. Lee, B. Chen, S. S. Yi, J. H. Jeong and L. R. Moorthy, *J. Am. Chem. Soc.*, 2010, 93, 494.
52. B. V. Ratnam, M. Jayasimhadri, K. Jang, H. S. Lee, S. S. Yi and J. H. Jeong, *J. Am. Ceram. Soc.*, 2010, 93, 3857.
53. Y. G. Su, L. P. Li and G. S. Li, *Chem. Mater.*, 2008, 20, 6060.
54. A. F. Kirby and F. S. Richardson, *J. Phys. Chem.*, 1983, 87, 2544.
55. M. L. Debasu, D. Ananias, A. G. Macedo, J. Rocha and L. D. Carlos, *J. Appl. Phys.*, 2011, 22, 3354.
56. Y. Liu, Z.G. Lu, Y. Y. Gu and W. Li, *J. Lumin.*, 2012, 132, 1220.
57. J. A. Dorman, J. H. Choi, G. Kuzmanich and J. P. Chang, *J. Phys. Chem. C.*, 2012, 116, 12854.

Citations here in the format A. Name, B. Name and C. Name, *Journal Title*, 2000, **35**, 3523; A. Name, B. Name and C. Name, *Journal Title*, 2000, **35**, 3523.